

Digital all-sky polarization imaging of partly cloudy skies

Nathan J. Pust and Joseph A. Shaw*

Department of Electrical and Computer Engineering, 610 Cobleigh Hall,
Montana State University, Bozeman, Montana 59717, USA

*Corresponding author: jshaw@montana.edu

Received 4 June 2008; accepted 6 August 2008;
posted 13 October 2008 (Doc. ID 96960); published 19 November 2008

Clouds reduce the degree of linear polarization (DOLP) of skylight relative to that of a clear sky. Even thin subvisual clouds in the “twilight zone” between clouds and aerosols produce a drop in skylight DOLP long before clouds become visible in the sky. In contrast, the angle of polarization (AOP) of light scattered by a cloud in a partly cloudy sky remains the same as in the clear sky for most cases. In unique instances, though, select clouds display AOP signatures that are oriented 90° from the clear-sky AOP. For these clouds, scattered light oriented parallel to the scattering plane dominates the perpendicularly polarized Rayleigh-scattered light between the instrument and the cloud. For liquid clouds, this effect may assist cloud particle size identification because it occurs only over a relatively limited range of particle radii that will scatter parallel polarized light. Images are shown from a digital all-sky-polarization imager to illustrate these effects. Images are also shown that provide validation of previously published theories for weak ($\sim 2\%$) polarization parallel to the scattering plane for a 22° halo. © 2008 Optical Society of America

OCIS codes: 120.5410, 260.5430, 290.1310, 280.0280.

1. Introduction

For clear skies, molecular (Rayleigh) scattering in the atmosphere polarizes visible light in directions perpendicular to the scattering plane—the plane that contains the Sun, the scattering object, and the observer. Previous and present research observes that cloud presence reduces the measured degree of linear polarization (DOLP) from that of the clear sky [1–3]. This DOLP reduction is caused primarily by multiple scattering within the cloud, which depolarizes the light. In spite of the reduced DOLP, in partly cloudy skies the angle of polarization (AOP) of light scattered from clouds often remains consistent with that of the clear sky [1,2,4]. This measured cloud AOP is not produced by the cloud itself, but instead represents the AOP of the polarized Rayleigh-scattered light in the path between the cloud and the observer—while light scattered from the cloud itself is effectively unpolarized.

Previous investigators have focused upon the observed consistencies between measured cloud AOP and clear-sky AOP and did not focus on observed deviations of cloud AOP from the clear-sky pattern [2]. However, we have observed many instances where cloud AOP exhibits departures from the clear-sky AOP. In this paper we present observations made under clear and partly cloudy conditions and identify several interesting cases where the images deviate from what might be expected from simple considerations of clear and cloudy conditions. In the process, we show what we believe is the first polarimetric evidence of a region of enhanced aerosol separating clouds from the clear sky, recently dubbed the “twilight zone” [5]. We also use a polarization image to provide support for previously published theories describing the polarization state of light in a 22° halo.

2. Polarization Images of Clear and Cloudy Skies

We previously described a dual-field, imaging polarimeter designed for studying both sky polarization and ground-based object polarization signatures

0003-6935/08/34H190-09\$15.00/0
© 2008 Optical Society of America

at visible and near-infrared wavelengths [1]. This polarimeter can be switched between two fields of view—a wide-angle fisheye field of view for imaging the full sky and a narrow field of view for imaging smaller objects. This instrument operates in five 10 nm bands defined by interference filters centered at 452, 491, 532, 632, and 701 nm. Two liquid-crystal variable retarders (LCVRs) are used to electronically vary the polarization sensitivity of the imager so that a full Stokes image is measured in less than a few tenths of a second at each wavelength. The resulting set of four intensity images from a CCD camera are inverted by a calibration matrix to form 4-element Stokes images [1,6]. This speed allows reliable measurements in partly cloudy skies without polarization artifacts that would arise when clouds move more than a small fraction of a pixel between frames.

The dual-field polarization imager used here builds upon and extends a varied legacy of sky-polarization imagers. North and Duggin [7] used a four-lens stereoscopic camera pointed down at a dome mirror to record all-sky polarization images from scanned film. Shortly thereafter, Lee [8] published an insightful discussion of sky-polarization images obtained from scanned film exposed through a manually rotated linear polarizer. Pomozi *et al.* [2] and Horvath *et al.* [3] have performed a wide variety of studies with an all-sky polarization imager that uses scanned film images recorded through linear polarizers. Voss and Liu [9] developed a digital all-sky-polarization imager that used rotating filter wheels to vary both polarization state and wavelength. Liu and Voss [10] used this system to explore the variation of clear-sky polarization with atmospheric optical depth and surface reflectivity. Recently, Cronin *et al.* [11] used a digital all-sky-polarization imager with a manually rotated linear polarizer to study sky-polarization patterns during twilight. Our liquid-crystal-based imager provides the advantages of previous digital imagers, and

also provides a speed advantage over systems that rely on time-sequential polarization images. The subsecond time required to gather a full set of four polarization images allows this system to measure sky polarization with variable clouds without polarization artifacts that arise when clouds move between images [1,6,11]. In the present study the instrument is used to study clear and partly cloudy sky polarization.

Figure 1 shows the 450 nm degree of linear polarization (DOLP) and angle of polarization (AOP), respectively, for a clear sky seen through the fisheye lens of our LCVR-based imaging polarimeter at 17:55 (Mountain Standard Time, MST = UTC –6 h) on 26 June 2006 from the top of the engineering building at Montana State University in Bozeman, Montana (45.67°N, 111.05°W). In the DOLP image, the band of maximum polarization caused by Rayleigh scattering is clearly visible in an arc positioned 90° from the Sun (with a maximum DOLP = 66%). Similar data are seen in the other four wavelength bands (not shown), with the longer wavelengths exhibiting higher maximum DOLP values. The oval at the top of the image is the Sun occulter, which prevents overexposure by direct sunlight. Also, penthouses on the top of the building can be seen to the top (west) and the top left (southwest). The black area below the occulter in the AOP image is the Babinet neutral point. This area has been denoted black because the AOP is undefined where the DOLP is equal to zero. The other black area to the right of the occulter is an area of overexposed reflection from a building antenna. It should be noted that AOP values in regions away from the image center are difficult to interpret because the fisheye lens projects a three-dimensional polarized sky dome onto a two-dimensional Stokes image. For reference, though, a 90° AOP measurement at the image center represents a vector oriented from left to right.

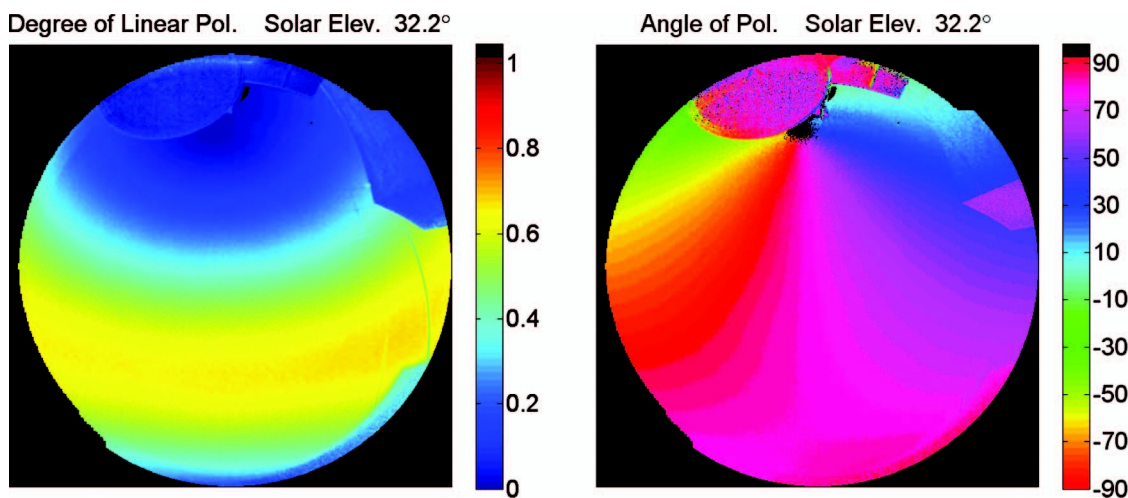


Fig. 1. Clear-sky polarization at 450 nm (26 June 2006, 5:55 pm MDT = UTC –6 h). Black areas denote regions that are overexposed, underexposed, uncalibrated, or—in the case of the AOP—undefined due to lack of measurable polarized light. For AOP to be considered defined, a threshold of DOLP > 1% was chosen.

A. Aerosol and Subvisual Cloud Influence on Polarization in Apparently Clear Sky

Figure 2 shows an image of a single cloud in an otherwise clear sky. The image was taken at the same time of day (early evening) as Fig. 1—but 3 days earlier. The DOLP is considerably lower for the cloud than for the clear sky, owing to the largely unpolarized light arising from multiple scattering in the cloud. The clear-sky DOLP is also reduced in this image compared to Fig. 1. While the exact cause of this reduction remains to be conclusively determined, the effect is consistent in images containing clouds. It is our feeling that unseen aerosols and possibly thin clouds in what has recently been called the “twilight zone” between a cloud and the clear sky [5,12,13] are reducing the DOLP in what appears to be clear sky. We believe that this effect on the sky polarization is directly related to the recently described observations of enhanced optical depth near clouds [5]. In partially cloudy skies, we see DOLP reductions in clear-sky areas between clouds that appear to be caused by subvisual aerosols and/or clouds. (Even though clouds appear to have hard edges, they are in fact surrounded by thin clouds.) Furthermore, these DOLP reductions show up in the clear sky long before we can physically see clouds in the sky.

Figure 3 shows this effect at 700 nm, but a very similar effect is seen at all of our observed wavelengths. The data from 11 September and 26 June demonstrate the typical progression of the maximum DOLP through a day with a clear sky. However, in the data from 23 June the maximum DOLP begins dropping away from the clear-sky curve around the solar elevation maximum (65.5° at 13:30 MST). Not until 3 h later (solar elevation angle = 41° at 16:30) are visible clouds seen in the imagery. We believe this drop in DOLP is caused by subvisual aerosols/clouds during cloud formation. Also, the long length of time (3 h) between the first DOLP drop and the appearance of visual clouds—indicated by

the gray area in Fig. 3—gives additional support to the recent claim that such subvisual clouds stretch tens of kilometers away from the visual clouds [5]. This effect is also seen after visible clouds leave the scene, indicated in the area following the gray-shaded period in Fig. 3. Therefore, we believe the polarimeter is seeing thin aerosol/cloud droplets that are not visible to the naked eye before and after clouds become visible to the eye.

In Fig. 2, it is notable that the cloud AOP does not deviate from the clear-sky AOP. This is typical when the clouds move through the band of maximum DOLP that is 90° from the Sun and when other clouds do not block the Sun. Nevertheless, many instances of cloud AOPs that depart from the clear sky have also been measured.

B. Observed Cloud AOPs that Depart from the Clear-Sky Polarization Pattern

Figure 4 shows an example of clouds that deviate from the AOP of the clear sky. Again, this image is taken at a similar afternoon time to Figs. 1 and 2—but a month earlier. As expected, the AOP in clear-sky areas between the clouds is similar to Figs. 1 and 2, but the AOP of several clouds in the image deviate from the clear-sky AOP. (Similar data are seen in 490, 530, and 630 nm images, but are not seen in the 450 nm image.) We assume that this is a liquid cloud based on its appearance. A regional radiosonde profile from Great Falls, Montana, suggested a cloud-base temperature between 0 and −5 °C, which is certainly reasonable for a liquid cloud. Also, for the 55–90° scattering angles of this cloud, single scatter models have consistently shown that cirrus ice crystals exhibit polarization angles that are in the same direction as for a clear sky—that is they are polarized perpendicular to the scattering plane [14–17]. If the bottom of the cloud was ice, its AOP would not be expected to follow the pattern discussed here.

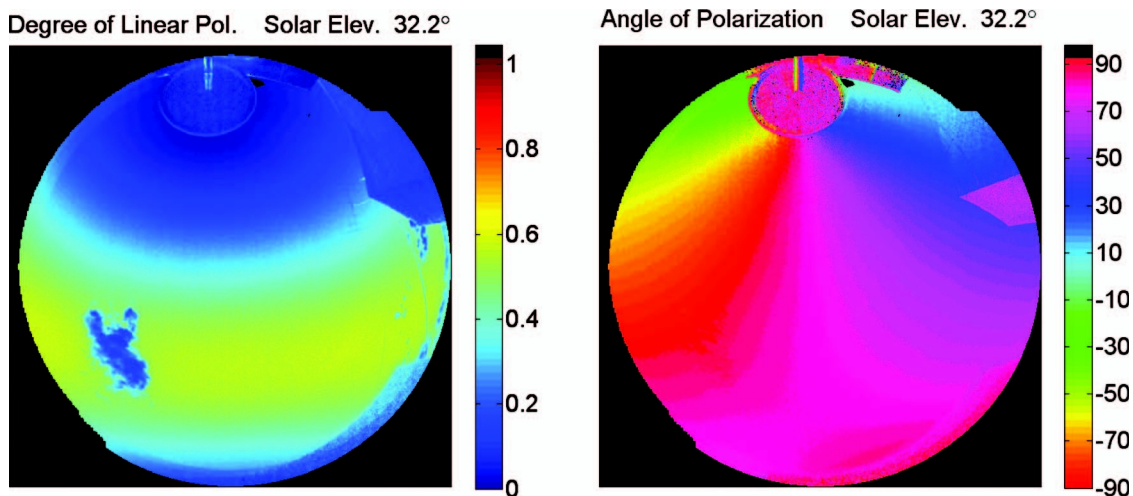


Fig. 2. Cloud polarization in a partially cloudy sky at 450 nm (23 June 2006, 5:55 pm MDT = UTC − 6 h). Black areas denote regions that are overexposed, underexposed, uncalibrated, or—in the case of the AOP—undefined due to lack of measurable polarized light. For AOP to be considered defined, a threshold of DOLP > 1% was chosen.

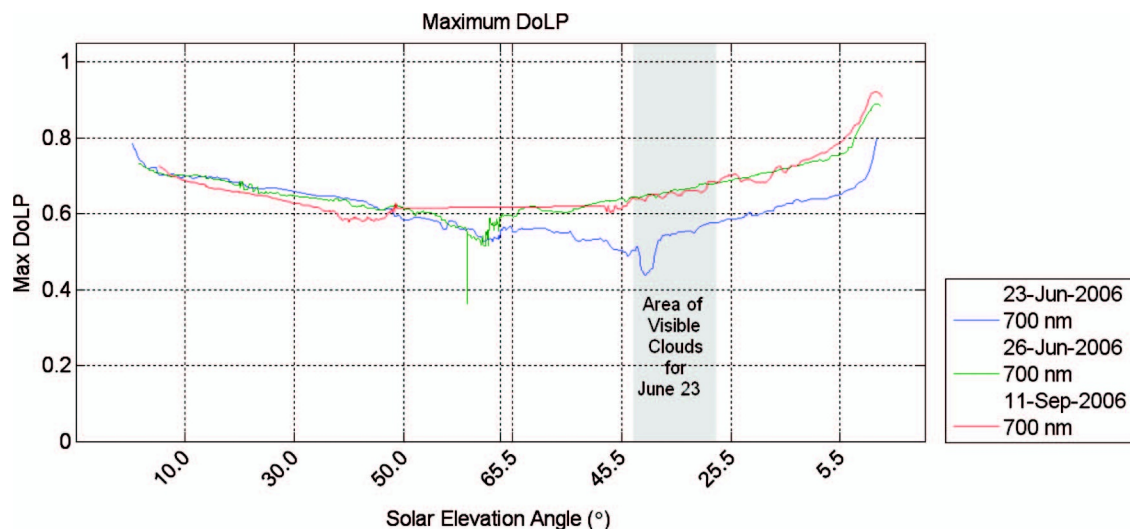


Fig. 3. Maximum degree of polarization for 23 June, 26 June, and 11 September 2006 at 700 nm. The sky was completely cloud free on 26 June and 11 September, while on 23 June the sky was perceived to be cloud free except in the gray-shaded time when a few small, localized clouds were visible (see Fig. 2). The flat spot in the graph of 11 September data occurs when the Sun never attained that height. The extra x -axis hash shows the maximum solar elevation for 23 June.

Several observations of Fig. 4 should be noted. First, the AOP throughout the image is either (1) identical to the clear-sky AOP, (2) oriented 90° from the clear-sky AOP, or (3) undefined. Up to the time of publication, this remains true for all data obtained by this imager. The AOPs have always remained within these three cases. Second, the clouds inside or near the band of maximum DOLP—at the bottom left in this image—exhibit little change from the clear-sky AOP. This is consistent in most images. It is rare for a cloud to show a change in the AOP when it is located in the high-DOLP band. Finally, the image shows many clouds in the vicinity of the Sun (behind the occulter). The Sun is most certainly partially blocked by these clouds. In all data taken by the imager, blocking of the Sun by clouds highly correlates to instances of cloud AOP changing from the

clear-sky AOP. Therefore, more clouds show changes in AOP relative to the clear sky when either (1) the Sun is obscured by clouds, or (2) the clouds are located in sky regions away from the band of high clear-sky DOLP. Other researchers have seen similar effects [2]. Reasons for each of these observations will be discussed in the next section.

3. Scattering Path Contributions to Measured Polarization

To better understand cloud AOP deviations from molecular-scattering AOP in a partly cloudy sky, it is important to consider individual contributions from the scattering path to the polarimetric imager. Figure 5 shows the independent scattering mechanisms that contribute to the polarimetric image, assuming an unpolarized source. First, Rayleigh

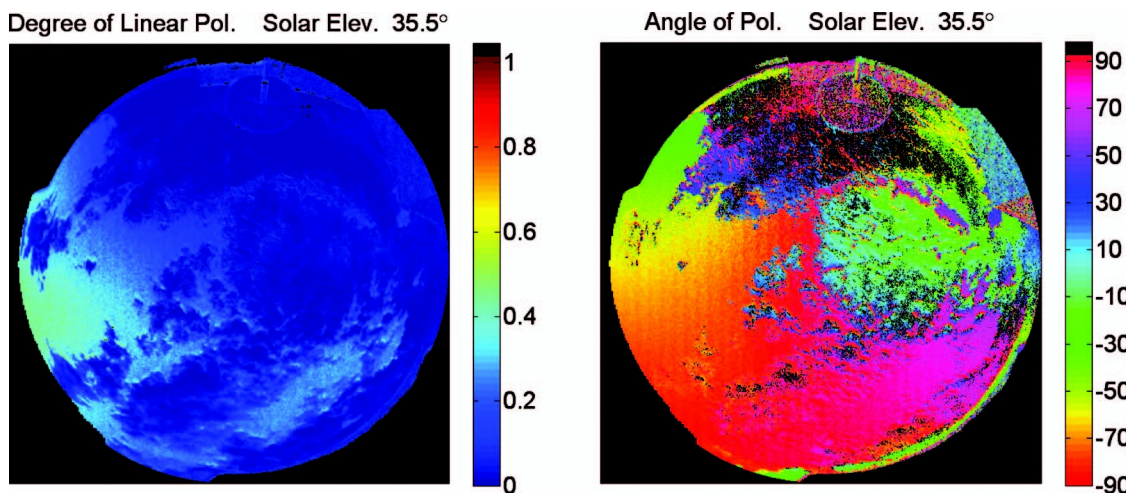


Fig. 4. Polarization for a cloud that changes the AOP at 700 nm (24 May 2006, 5:21 pm MDT = UTC - 6 h). Black areas denote regions that are overexposed, underexposed, uncalibrated, or—in the case of the AOP—undefined due to lack of measurably polarized light. For AOP to be considered defined, a threshold of DOLP $> 1\%$ was chosen.

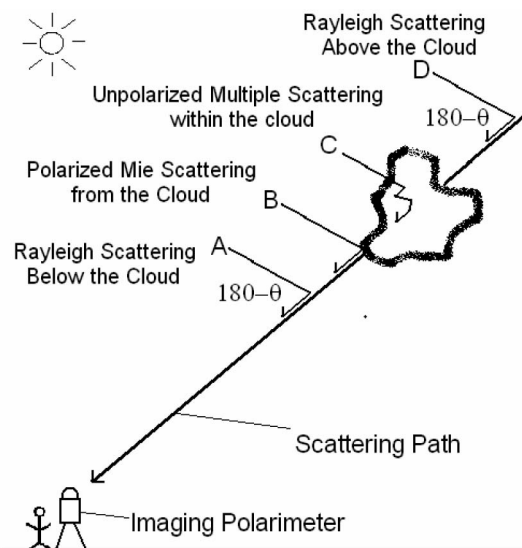


Fig. 5. Scattering contributors to the polarimetric ground measurement. The plane of the paper is the scattering plane. The polarized portion of the Rayleigh scattered components (**A** and **D**) is always polarized perpendicular to the scattering plane, while the polarized component of the Mie scattering from the cloud can potentially be polarized either parallel or perpendicular to the scattering plane. θ is the scattering angle. ($\theta = 0$ is forward scattering.)

scattering below the cloud (denoted **A** in Fig. 5) introduces light into the path. This light contains a component that is polarized perpendicular to the scattering plane—the plane including the Sun, the scattering object, and the observer—and a component that is unpolarized. (For Fig. 5, the scattering plane is the plane of the paper.)

Second, the polarized component of the light from the cloud consists of light that is both singly and multiply scattered (denoted **B** in Fig. 5). Single-scattered light from liquid clouds will be polarized either perpendicular or parallel to the scattering plane—depending upon cloud parameters such as drop size and cloud optical depth. Previous research has shown that most polarization from the cloud arises from single scattering, while multiply scattered light primarily reduces the DOLP [18]. Models have shown that, in the vast majority of cases, the AOP of the multiply scattered light is the same as the AOP of the singly scattered light [19,20]. Therefore, the polarized component of the light scattered by the cloud nominally will be polarized either parallel or perpendicular to the scattering plane.

Third, an unpolarized component of multiple scattering emanates from the cloud (denoted **C** in Fig. 5). Although this component is not strictly physically separate from the polarized component of the cloud radiance, conceptually it is helpful to consider it independently from the polarized component.

Finally, perpendicularly polarized Rayleigh scattering above the cloud (denoted **D** in Fig. 5) may contribute to the measurement. For thick clouds, it is not necessary to consider the molecular

scattering above the cloud because multiple scattering in the cloud destroys it. Still, for thin clouds it may contribute significantly to the polarimetric image.

The DOLP and AOP of the measured light depend upon the relative magnitudes of each of these components. The following paragraphs describe five common cases:

1. The unpolarized light from multiple scattering inside the cloud (**C**) severely dominates the brightness of the other components. Any polarized component from the other contributors (**A**, **B**, and possibly **D**) is so small that it remains below the detectable limit of the instrument. In this case, the instrument will measure unpolarized light (DOLP = 0) with an undefined AOP.

2. If the polarized component of the cloud scattering (**B**) is perpendicular to the scattering plane, then the polarimeter will only see polarization that is oriented perpendicular to the scattering plane (from components **A**, **B**, and possibly **D**). For this case, the measured DOLP will be reduced from the clear-sky value by the unpolarized component from the cloud (**C**), while the AOP of the polarimetric image will be in the same direction as the clear-sky AOP.

3. If the polarized component of the cloud scattering (**B**) is polarized parallel to the scattering plane, but is *dimmer* than the perpendicularly polarized Rayleigh scattered components (**A** and **D**), then the polarized component of the cloud will reduce the polarized component of the Rayleigh scattering. The polarized component of the cloud effectively depolarizes the stronger perpendicularly polarized Rayleigh scattering. In this case, the polarimeter measures a clear-sky DOLP component that is reduced by both the polarized component of the cloud and the unpolarized component from the cloud, but the AOP remains oriented in the same direction as the light scattered from the surrounding clear sky.

4. If the polarized component of the cloud scattering (**B**) is parallel to the scattering plane, and is *equal* in brightness to the Rayleigh scattered components that are polarized perpendicular to the scattering plane, then the polarized Rayleigh components (**A** and **D**) and the polarized cloud component (**B**) will cancel each other. The imager will measure completely unpolarized light.

5. Finally, if the polarized component of the cloud (**B**) is parallel to the scattering plane, but is *brighter* than the polarized Rayleigh-scattered components above and below the cloud, then the parallel-polarized cloud polarization will dominate the polarization of the Rayleigh scattering above and below the cloud (**A** and **D**). In this case, the AOP will be measured parallel to the scattering plane—or 90° from the clear-sky case, while the instrument will measure a cloud DOLP that is reduced by both the perpendicularly polarized Rayleigh scattering above and below the cloud and the unpolarized component of light scattered by the cloud.

It should be apparent that for many observations where clouds exhibit the same polarization as the clear sky, the observed AOP does not arise from the cloud itself but instead is produced by the Rayleigh scattered light in the atmospheric column between the observer and the cloud.

For all the above cases, the AOP is theoretically either the same as the clear sky, 90° from the clear sky, or undefined. The observed AOP depends upon the relative amplitudes of each scattering component. For cases where the Rayleigh scattered components dominate, the AOP is consistent with that of the clear sky. For cases where the polarized cloud component dominates, the AOP can at times be 90° from the clear sky (depending upon the polarization direction of the cloud droplet scattering).

Case 5 explains why it is more common to observe AOP changes from the clear sky when either the Sun is blocked by clouds, or the clouds are positioned away from the band of increased clear-sky DOLP. In these cases, either the total Rayleigh scattering below the cloud is reduced—as when the Sun is blocked—or the polarized Rayleigh scattering is low—as when the cloud is away from the maximum DOLP band. Both cases reduce the polarized Rayleigh scattered light in the column below the cloud, allowing the parallel-polarized cloud light to become brighter than the perpendicularly polarized component of the Rayleigh scattered light. In these cases, a measurable change in AOP of the cloud from that of the clear sky occurs. In contrast, it is rare for a cloud to show a change in AOP from the clear sky when either the column below the cloud is fully lit by the Sun or the cloud is near the maximum

clear-sky polarization band. In these cases the polarized Rayleigh scattered component has a larger magnitude—and is thus more difficult to overcome by the polarized cloud component (Case 3).

Case 5 describes the unique conditions that must exist for measured AOP of a cloud to be different than the clear sky. In this case, the polarized component of cloud scattering is larger than the polarized Rayleigh scattering. This case predicts that the AOP will be oriented 90° from the surrounding clear-sky AOP. As can be seen in Fig. 6, the AOP imagery agrees perfectly with this prediction. There is clearly a 90° shift between the cloud and the surrounding clear sky.

It should be noted that this treatment ignores the case of secondary illumination of both the cloud and the column beneath the cloud by other surrounding clouds. If the Sun was adequately blocked and another cloud illuminated the column, the AOP could potentially change (this would be a special case of multiple scattering). If this were the case, the AOP would shift from one of the three expected values (0° from the clear-sky AOP, 90° from the clear-sky AOP, or undefined). Since all data observed thus far have shown AOPs that fall within the three expected values, we are confident that the issue of secondary illumination is sufficiently small to be neglected in this treatment.

4. Cloud Droplet Size Estimation

For liquid clouds that change the AOP, it is clear that the scattering processes in the cloud scatter light that is predominantly polarized parallel to the scattering plane. Our data suggest that—although it is

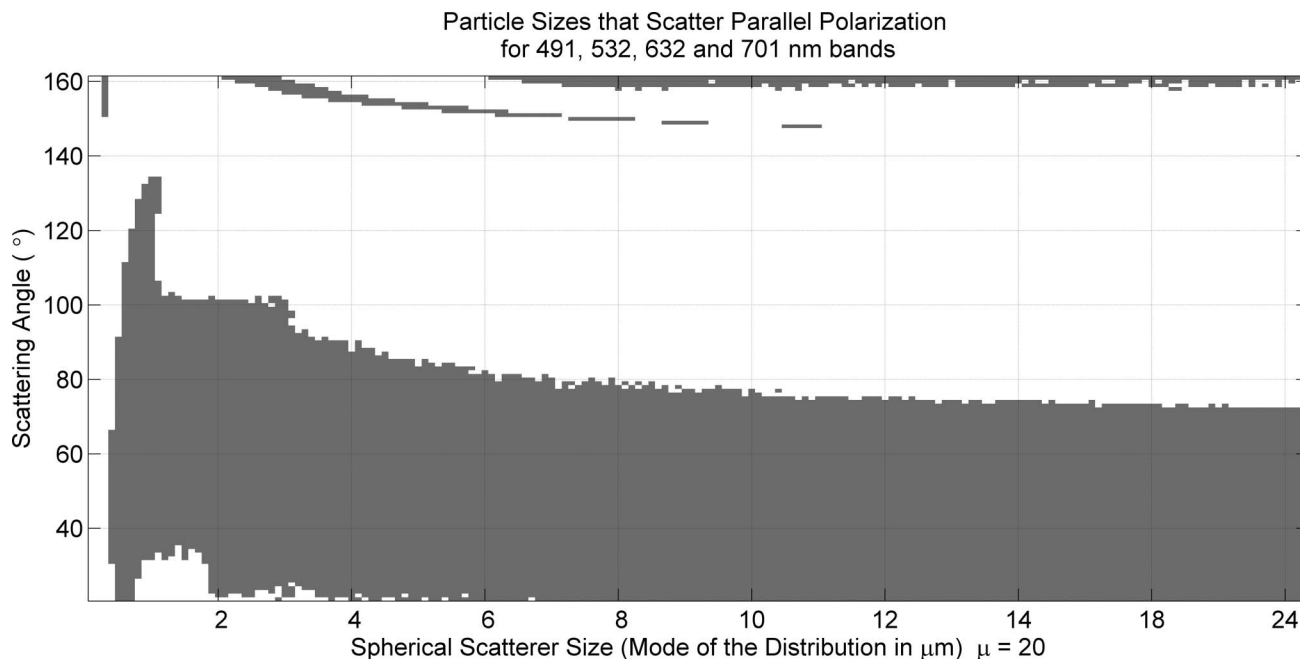


Fig. 6. Areas of spherical particle sizes that scatter a polarization that is parallel to the scattering plane (shown in the gray areas). The mode radius of the cloud droplet size distribution (the most frequent radius size of the distribution) is labeled on the x axis. (Distribution parameter $\mu = 20$.)

difficult to obtain a magnitude of the scattering from the cloud—the polarization angle of the scattering itself may provide information about the droplet size distribution composing the cloud. Although researchers have used polarization from satellite and airborne measurements to retrieve liquid cloud parameters [21–23], to our knowledge this has not been done with ground-based sky-polarization imager data. To demonstrate the feasibility of this technique, we assumed that the polarization primarily arises from single scattering within the cloud and ran several single-scatter Mie models to find droplet sizes that scattered light polarized parallel to the scattering plane.

For each of the bands of the imager, Mie scattering results were obtained over 5 wavelength samples across the band and then averaged to account for wavelength dispersion in the scattering. The index of refraction of the water was taken to be $n = 1.33$. The cloud droplet distribution function was selected to be a gamma distribution following Kokhanovsky [18]. The parameter μ was selected to be 20, 10, 5, and 1. (This parameter is inversely related to the width of the droplet distribution. $\mu = 20$ represents a narrow distribution, while $\mu = 1$ is a wide distribution.) The number of particles used was 50. They were sequentially selected from a random gamma distribution of 1000 that had been sorted. (This ensured that the distribution was representative, but still had some random attribute.)

For each wavelength, a mapping of droplet distributions that scattered a parallel polarization was calculated for scattering angles from 20 to 160°. Since the AOP deviation from the clear sky in Fig. 4 was observed not only in the 700 nm band, but also at 630, 530, and 490 nm (not shown), cloud droplet radii

that would scatter parallel polarization for all of these 4 bands were mapped. The areas where the droplet distributions would scatter parallel polarization are shown as gray in Fig. 6 (for a distribution of $\mu = 20$). The mode of the distributions (most frequent drop size) is plotted on the x axis.

Variation in the width of the distribution function did not appreciably affect the data except that large distributions further limited the set of particle sizes that could scatter parallel polarization. In other words, a narrow cloud droplet size distribution can scatter parallel polarization for a larger set of mean particle sizes than a wide distribution. To include the most possible size distributions, the $\mu = 20$ plot is shown in Fig. 6. (To show that the dependence on μ is relatively insignificant, Fig. 7 is also provided for $\mu = 5$.)

Figure 6 shows that for small scattering angles a departure of measured cloud AOP from the clear-sky AOP does not give any useful information about mean droplet size. Many different droplet distributions can give the parallel AOP signature. Still, for large scattering angles (80–130°), an AOP departure from the clear-sky value indicates that the mean drop size must be below $7\text{ }\mu\text{m}$. In the example data shown in Fig. 4, only the green colored clouds on the far right of the image would have scattering angles this small. The scattering angles for these clouds would be roughly 80–90°. Therefore, the mode cloud droplet size for this particular cloud must be between 0.5 and $7\text{ }\mu\text{m}$. This method shows potential to provide auxiliary cloud droplet information. Still, further investigation with other instruments is needed to validate this method for a larger cloud data set.

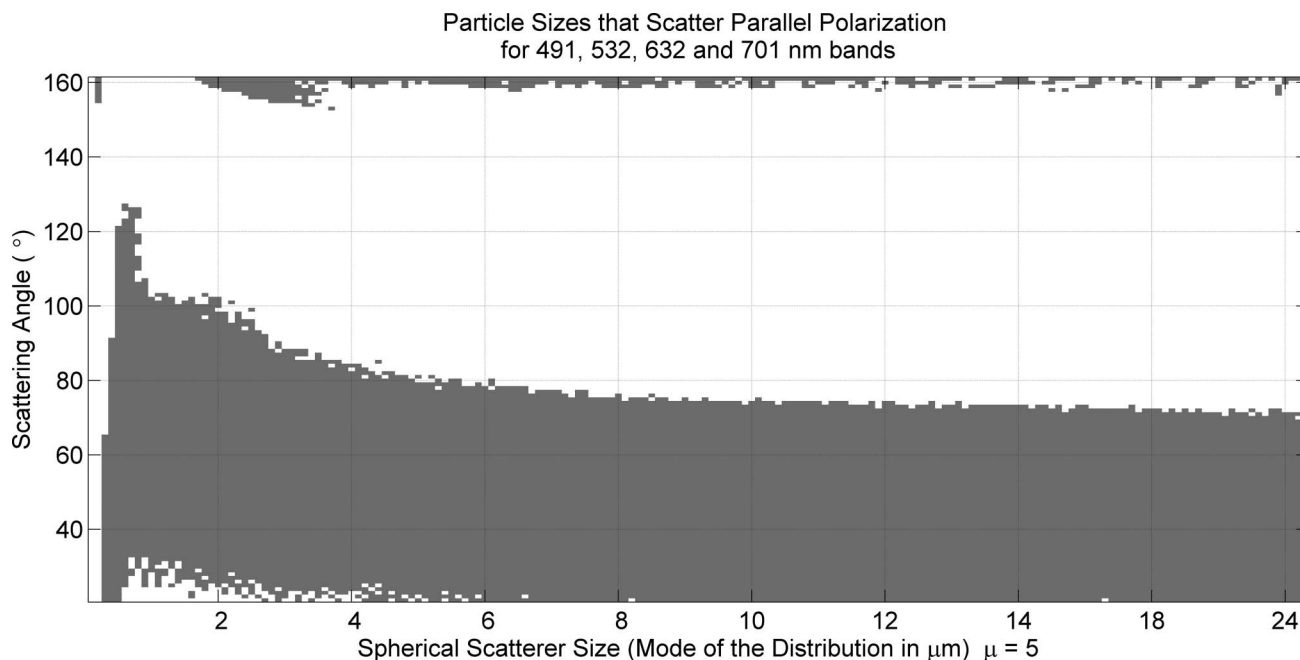


Fig. 7. Same as Fig. 6 but with a wider cloud droplet distribution function ($\mu = 5$).

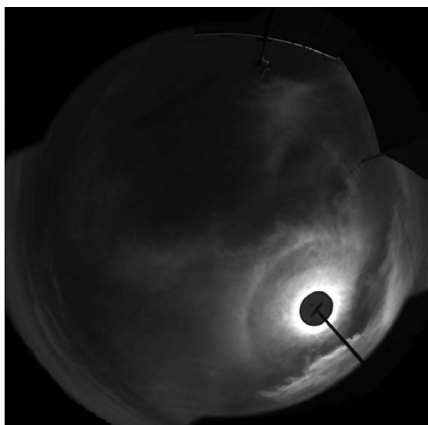


Fig. 8. Intensity image of a 22° halo at 11:24:13 MDT = UTC - 6 on 12 April 2006 (450 nm).

5. Halo Polarization

On 24 April 2006 we obtained polarimetric images of a 22° halo within a sequence of cloud images. Figures 8 and 9 show images taken of the halo at 450 nm. (The Sun occulter covers the Sun.) Although the halo was not complete in any of the images taken, these images show similar results to previous researchers [24–26]. These data provide further confirmation of previous theoretical predictions and measurement, which show that the 22° halo is polarized parallel to the scattering plane [24,25]. Like the clouds shown in Fig. 4, the halo AOP is parallel to the clear sky behind it. This is shown in Fig. 9 and other wavelengths show similar AOP. For many images, though, the DOLP became low and noisy due to variation in brightness from the cloud structure in the image. Even so, none of the halo data exhibited DOLPs greater than 2%. This was consistent with previous investigators [24,25]. It should be noted that the method used previously to constrain the liquid cloud droplet sizes (shown in Fig. 4) cannot be used for the halo since in this case the cloud particles are ice crystals.

6. Conclusion

We have shown examples of clear and cloudy sky polarization images measured with a fisheye imager that is capable of recording full digital Stokes-vector sky images rapidly enough to avoid polarization errors in rapidly changing sky conditions. The images show that there is significantly reduced maximum DOLP in apparently clear regions of sky when even one small cloud is present elsewhere in the sky, relative to what is observed in a truly clear sky. This effect is observed for multiple hours before a cloud becomes visible and for multiple hours after a cloud disappears, lending support to recent reports of higher optical depth from aerosols and subvisual clouds in what has been called the “twilight region” between clouds where the sky is not truly clear.

While many of our measurements show that the AOP is unchanged beneath a cloud, we have also shown images where the cloud significantly changes the AOP from that of the immediately adjacent clear sky. Whether a cloud changes or retains the clear-sky AOP depends on the polarization state of light scattered from the cloud (i.e., whether the cloud is composed of liquid or ice) and on the relative brightness of the light scattered by the cloud, the light transmitted through the cloud, and the light scattered below the cloud. For liquid clouds this effect can be used to assist in cloud droplet size retrieval.

Finally, images of a 22° halo provide validation of previously published theories for halo polarization. Our measurements show that the halo is linearly polarized parallel to the scattering plane, with a DOLP of 2% or less.

This material is based on research sponsored by the Air Force Research Laboratory, under agreement number FA9550-07-1-0011. The U.S. Government is authorized to reproduce and distribute reprints for Governmental purposes notwithstanding any copyright notation thereon. The views and conclusions contained herein are those of the authors and should

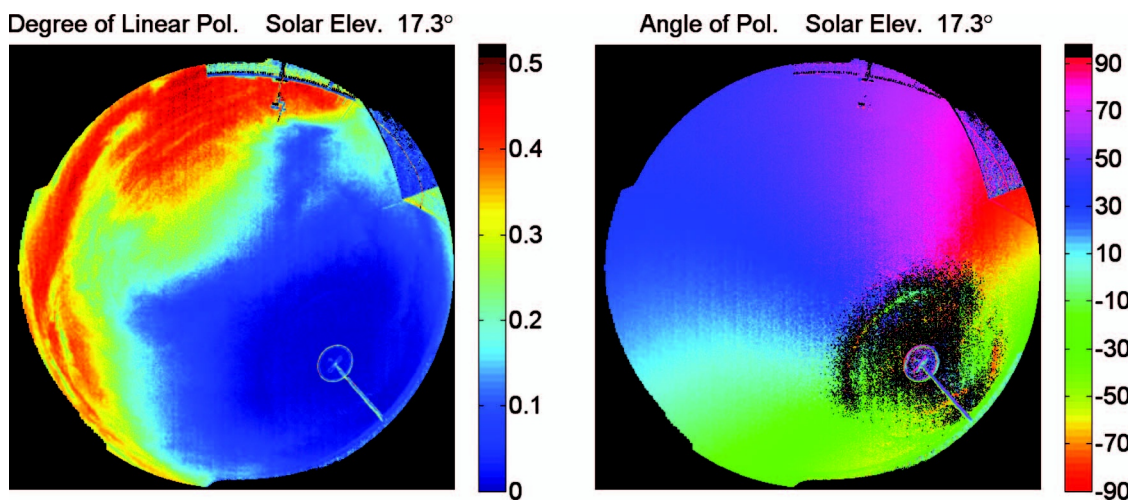


Fig. 9. DOLP and AOP images of a 22° halo at 11:24:13 MDT = UTC - 6 on 12 April 2006 (450 nm). Areas of low DOLP (1%) are masked in black. Black areas denote regions that are overexposed, underexposed, uncalibrated, or—in the case of the AOP—undefined owing to the lack of measurably polarized light. For AOP to be considered defined, a threshold of DOLP > 1% was chosen.

not be interpreted as necessarily representing the official policies or endorsements, either expressed or implied, of the Air Force Office of Scientific Research or the U.S. Government.

References

1. N. J. Pust and J. A. Shaw, "Dual-field imaging polarimeter using liquid crystal variable retarders," *Appl. Opt.* **45**, 5470–5478 (2006).
2. I. Pomozi, G. Horvath, and R. Wehner, "How the clear-sky angle of polarization pattern continues underneath clouds: full-sky measurements and implications for animal orientation," *J. Exp. Biol.* **204**, 2933–2942 (2001).
3. G. Horvath, A. Barta, J. Gal, B. Suhai, and O. Haiman, "Ground-based full-sky imaging polarimetry of rapidly changing skies and its use for polarimetric cloud detection," *Appl. Opt.* **41**, 543–559 (2002).
4. M. L. Brines and J. L. Gould, "Skylight polarization patterns and animal orientation," *J. Exp. Biol.* **96**, 69–91 (1982).
5. I. Koren, L. A. Remer, Y. J. Kaufman, Y. Rudich, and J. V. Martins, "On the twilight zone between clouds and aerosols," *Geophys. Res. Lett.* **34**, L08805 (2007).
6. J. S. Tyo, D. L. Goldstein, D. B. Chenault, and J. A. Shaw, "Review of passive imaging polarimetry for remote sensing applications," *Appl. Opt.* **45**, 5453–5469 (2006).
7. J. A. North and M. J. Duggin, "Stokes vector imaging of the polarized sky-dome," *Appl. Opt.* **36**, 723–730 (1997).
8. R. L. Lee, Jr., "Digital imaging of clear-sky polarization," *Appl. Opt.* **37**, 1465–1476 (1998).
9. K. J. Voss and Y. Liu, "Polarized radiance distribution measurements of skylight. I. System description and characterization," *Appl. Opt.* **36**, 6083–6094 (1997).
10. Y. Liu and K. J. Voss, "Polarized radiance distribution measurement of skylight. II. Experiment and data," *Appl. Opt.* **36**, 8753–8764 (1997).
11. T. W. Cronin, E. J. Warrant, and B. Greiner, "Celestial polarization patterns during twilight," *Appl. Opt.* **45**, 5582–5589 (2006).
12. A. Marshak, G. Wen, J. A. Coakley, Jr., L. A. Remer, N. G. Loeb, and R. F. Cahalan, "A simple model for the cloud adjacency effect and the apparent bluing of aerosols near clouds," *J. Geophys. Res.* **113**, D14S17 (2008), doi:10.1029/2007JD009196.
13. I. Koren, L. Oreopoulos, G. Feingold, L. A. Remer, and O. Altaratz, "How small is a small cloud," *Atmos. Chem. Phys. Discuss.* **8**, 6379–6407 (2008).
14. P. Goloub, M. Herman, H. Chepfer, J. Riedl, G. Brogniez, P. Couvert, and G. Seze, "Cloud thermodynamical phase classification from the POLDER spaceborne instrument," *J. Geophys. Res.* **105**, 14747–14759 (2000).
15. Y. Takano and K. N. Liou, "Radiative transfer in cirrus clouds. Pt. III: Light scattering by irregular ice crystals," *J. Atmos. Sci.* **52**, 818–837 (1995).
16. A. Macke, J. Mueller, E. Raschke, "Single scattering properties of atmospheric ice crystals," *J. Atmos. Sci.* **53**, 2813–2825 (1996).
17. L. C. Labonnote, G. Brogniez, J. C. Buriez, and M. Doutriaux-Boucher, "Polarized light scattering by inhomogeneous hexagonal monocrystals: validation with ADEOS-POLDER measurements," *J. Geophys. Res.* **106**, 12139–12155 (2001).
18. A. Kokhanovsky, "Optical properties of terrestrial clouds," *Earth Sci. Rev.* **64**, 189–241 (2004).
19. G. W. Kattawar and G. N. Plass, "Degree and direction of polarization of multiple scattered light. 1: homogeneous cloud layers," *Appl. Opt.* **11**, 2851–2865 (1972).
20. K. N. Liou, *An Introduction to Atmospheric Radiation* (Academic, 1980).
21. F. M. Breon and P. Goloub, "Cloud droplet effective radius from spaceborne polarization measurements," *Geophys. Res. Lett.* **25**, 1879–1882 (1998).
22. A. A. Kokhanovsky, "The determination of the effective radius of drops in water clouds from polarization measurements," *Phys. Chem. Earth B* **25**, 471–474 (2000).
23. W. G. Egan, S. Israel, M. Sidran, E. E. Hindman, W. R. Johnson, and V. S. Whitehead, "Optical properties of continental haze and cumulus and orographic clouds based on space shuttle polarimetric observations," *Appl. Opt.* **32**, 6841–6852 (1993).
24. G. P. Konnen, "Polarization and intensity distributions of refraction halos," *J. Opt. Soc. Am.* **73**, 1629–1640 (1983).
25. G. P. Konnen and J. Tinbergen, "Polarimetry of a 22° halo," *Appl. Opt.* **30**, 3382–3400 (1991).
26. D. Lynch, "Polarization models of halo phenomena I. The parhelic circle," *J. Opt. Soc. Am.* **69**, 1100–1102 (1979).